Equilibrium Theory for Simulated Moving Bed Adsorption Processes

Anthony S. T. Chiang
Dept. of Chemical Engineering, National Central University, Chung-Li, Taiwan, ROC 32054

The steady-state operation of a simulated moving bed (SMB) process can be modeled by that of an equivalence true countercurrent (TCC) adsorption unit. An equilibrium theory based on the TCC unit is very useful for the selection of a proper condition to operate an SMB process. The exact analysis of such an equilibrium model, however, has been limited to systems following a constant selectivity stoichiometric isotherm, which is not frequently observed. In this article, the equilibrium theory was extended to a multicomponent system that follows a constant selectivity nonstoichiometric isotherm. An exact solution is presented for the complete separation regions on the parameter space. The analysis is further applied to cases where only partial separation can be achieved.

Introduction

Simulated moving bed (SMB) adsorption processes have been used to solve many important industry separation problems. A model is thus needed for their design and operation. One way to model an SMB process is to consider, instead, an equivalent true countercurrent (TCC) adsorption unit (Hotier, 1996; Ruthven and Ching, 1989). To further simplify the case, one can assume that this equivalent TCC unit is operated under local equilibrium condition. Such an equilibrium model has been the basis for the recent works of Storti et al. (1989, 1993, 1995) and Mazzotti et al. (1994, 1996, 1997).

Under the equilibrium model, there are four operation parameters involved in the four-section TCC unit showed in Figure 1. These operation parameters can be identified as the net fluid to solid flow ratios m_1 to m_4 in the sections. These ratios can further be related to the normalized port switching time of the corresponding SMB process through geometric and kinematic equivalencies (Storti et al., 1995).

The equilibrium model could be reduced to a set of algebraic equations if the adsorption follows a constant selectivity stoichiometric isotherm. Storti et al. (1993) shows that one can identify a range of operation conditions such that the feed components are split into two groups leaving, respectively, from the raffinate and the extract outlets.

To achieve such a complete separation, the fluid to solid flow ratio m_1 must be large enough to completely regenerate the solid stream before it is recycled. The flow ratio m_4 must be low enough to adsorb all raffinate components from the recycled desorbent. Above that, the flow ratios m_2 and m_3 must also be limited in a region on the parameter space (Mazzotti et al., 1994). For binary separation systems, exact solution to define the complete separation condition on the m_2-m_3 space has been given by Storti et al. (1993). The analysis has recently been extended to multicomponent systems by Chiang (1998).

The results discussed above are, however, limited to cases where all components have the same saturation capacity. This

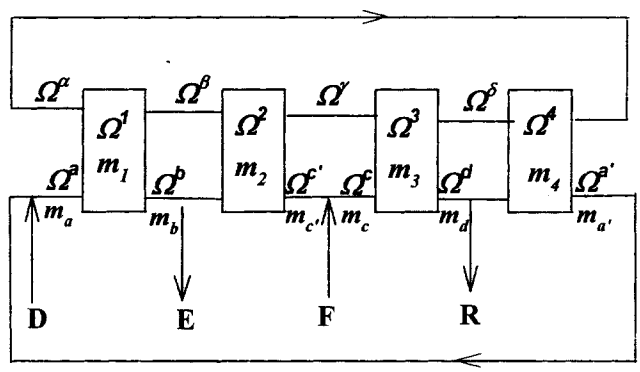

Figure 1. Equivalent TCC adsorption unit to model the SMB process.

System variables involved are as indicated.

is a rather artificial assumption. Mazzotti et al. (1996) have tried to remove this assumption with a nonstoichiometric Langmuir isotherm. Nevertheless, a constant fluid velocity had to be assumed to solve the model even numerically.

Storti et al. (1995) further demonstrated that one can identify more than the complete separation region. Closed regions on the m_2-m_3 parameter space exist that lead to different separation results. For example, a clean extract output might be produced with a contaminated raffinate output or the reverse case. Again, the analysis was made on a binary separation system. However, the existence of such regions should be general.

Two aspects of the equilibrium theory will be discussed here. First, the technique previously developed to solve the equilibrium model for multicomponent systems under a constant selectivity stoichiometric isotherm will be extended to systems following a nonstoichiometric isotherm. To do so, a thermodynamic consistent Gurvitsch isotherm is employed instead of the Langmuir isotherm used by Mazzotti et al. (1996). Then, the same technique will be employed to solve for cases where only partial separation can be achieved. With such solutions, the m_2-m_3 parameter space can be divided into regions of different separation results. Finally, the example problem discussed by Mazzotti et al. (1996) will be tested with the new approach.

Equilibrium Theory

Adsorption isotherms

The Langmuir isotherm

$$\theta_i \equiv \frac{\Gamma_i}{\Gamma_i^\infty} = \frac{K_i \rho_f y_i}{1 + \sum_{j=2}^{N} K_j \rho_f y_j}, \quad \text{for } i = 2, N \tag{1}$$

is frequently used to describe the adsorption of components in a chromatographic separation process. An important feature of this isotherm is that the fractional coverages θ_i for $i = 2, N$ do not sum up to one. This is perfectly legal since component 1, the eluent, is usually in large excess or adsorbed very weakly and has not been included in the above isotherm equation.

For a bulk separation SMB process, all components in the system must be considered as adsorptive. If the process is operated under liquid phase, the Gurvitsch's rule (Gurvitsch, 1915), that is, $\Sigma\, \Gamma_i \Gamma_i^\infty = 1$, should in general be true. One may have a constant selectivity system if the free energy of immersion is independent of the adsorbed phase composition (Minka and Myers, 1973).

If a bulk separation SMB process is operated under vapor phase, the influence of spreading pressure on the adsorbed phase activity coefficients may sometimes be neglected (Rota et al., 1993). This means $\Sigma\, \Gamma_i/\Gamma_i^0 \equiv 1$ where Γ_i^0 is the adsorption of pure component i at the system spreading pressure (Talu et al., 1995). Rota et al. (1993) have further suggested that $\Gamma_i^0 \equiv \Gamma_i^\infty$ if all components in the system are strongly adsorbed, as is frequently the case.

According to the above arguments, a Gurvitsch isotherm

$$\theta_i \equiv \frac{\Gamma_i}{\Gamma_i^\infty} = \frac{K_i \rho_f y_i}{\sum_{j=1}^{N} K_j \rho_f y_j} = \frac{K_i \rho_f y_i}{\delta_G}, \quad \text{for } i = 1, N \tag{2}$$

may be another choice of the adsorption isotherm to model an SMB process.

Notice that if $y_1 \equiv 1$, one can normalize the K_i $(i = 2, N)$ in Eq. 2 by $K_1 \rho_f$. After that, the Gurvitsch isotherm will be the same as the isotherm (Eq. 1) for components $i = 2, N$. In other words, an SMB chromatographic separation process that follows isotherm (1) can be considered as a Gurvitsch system if one assumes the adsorption of the eluent is $\theta_1 = 1 - \sum_{i=2}^{N} \theta_i$. Therefore, all following discussions concerning the Gurvitsch isotherm also apply to such an SMB chromatographic separation system.

As we have mentioned, Mazzotti et al. (1996) took a Langmuir isotherm in their equilibrium model to deal with nonstoichiometric systems. The isotherm employed by Mazzotti et al. (1996) was similar to Eq. 1, but the component indices were allowed to run from 1 to N, that is,

$$\theta_i \equiv \frac{\Gamma_i}{\Gamma_i^\infty} = \frac{K_i \rho_f y_i}{1 + \sum_{j=1}^{N} K_j \rho_f y_j} \equiv \frac{K_i \rho_f y_i}{\delta_L}, \quad \text{for } i = 1, N \tag{3}$$

This was considered as a general isotherm from which special cases such as the linear isotherm and the constant selectivity stoichiometric isotherm could be deduced. The linear isotherm could be obtained when the summation in the denominator is much less than 1. The constant selectivity stoichiometric isotherm could be obtained if $\Gamma_i^\infty = \Gamma^\infty$, and the summation in the denominator is much larger than 1.

The isotherms of Eqs. 3 and 2 are different in general, unless $\delta_L \approx \delta_G \gg 1$. We shall see that the equilibrium model is easier to solve under the isotherm of Eq. 2 than under Eq. 3.

ω-transformation

Whether the equilibrium is described by isotherm 2 or 3, a ω-transformation (Rhee et al., 1971, 1989) can always be applied to map the equilibrium compositions to a Ω-vector.

Given y_i, and thus θ_i, for an equilibrium system following isotherm 3, the components of the Ω-vector can be found as the roots to the equation

$$1 - \sum_{i=1}^{N} \frac{\gamma_i \theta_i}{\gamma_i - \omega} \equiv \prod_{i=1}^{N} \left(\frac{\Omega_i - \omega}{\gamma_i - \omega} \right) = 0 \tag{4}$$

In here $\gamma_i \equiv K_i \rho_s \Gamma_i^\infty$ is a normalized selectivity and ρ_s is the density of the adsorbent. It can be proved that Eq. 4 has N roots, and they satisfy the relation

$$0 \le \Omega_1 \le \gamma_1 \le \Omega_2 \le \gamma_2 \le \Omega_3 \ldots \le \gamma_{N-1} \le \Omega_N \le \gamma_N \tag{5}$$

γ_i will be taken as a component of the Ω-vector if and only if $y_i = \theta_i = 0$.

The mapping between the fractional coverages θ_i and the Ω-vector is one-to-one. Given Ω_1 to Ω_N, one can always find θ_i and vice versa. The mapping between θ_i and $\rho_f y_i$ is also one-to-one. We have

$$\rho_f = \left(\sum_{i=1}^{N} \theta_i/K_i\right) \Big/ \left(1 - \sum_{j=1}^{N} \theta_j\right) \tag{6}$$

$$y_i = \left(\frac{\theta_i}{K_i}\right) \Big/ \left(\sum_{j=1}^{N} \theta_j/K_j\right) \tag{7}$$

For the system following the Gurvitsch isotherm (Eq. 2), the same ω transformation can also be applied. However, a different Ω vector will be obtained. For this case, there are only $N-1$-independent θ_i; therefore, the corresponding Ω-vector has only $N-1$ components. They are again the roots to the equation

$$1 - \sum_{i=1}^{N} \frac{\gamma_i \theta_i}{\gamma_i - \omega} \equiv \left(\frac{-\omega}{\gamma_1 - \omega}\right) \prod_{i=2}^{N} \left(\frac{\Omega_i - \omega}{\gamma_i - \omega}\right) = 0 \tag{8}$$

and γ_i is a component of the Ω-vector if and only if $y_i = \theta_i = 0$. For the Gurvitsch isotherm, the $N-1$ components of the Ω-vector obey the relation

$$\gamma_1 \le \Omega_2 \le \gamma_2 \le \Omega_3 \ldots \le \gamma_{N-1} \le \Omega_N \le \gamma_N \tag{9}$$

Given Ω_2 to Ω_N for a Gurvitsch system, the fractional coverages can be found by

$$\theta_i = \frac{\prod_{j=2}^{N} (\gamma_i - \Omega_j)}{\prod_{\substack{j=1 \\ j \ne i}}^{N} (\gamma_i - \gamma_j)} \tag{10}$$

A one-to-one mapping between θ_i and y_i also exists. Therefore, the ω-transformation for the Gurvitsch isotherm (Eq. 2) is an $N-1$ dimensional mapping, while that for isotherm 3 is an N-dimensional mapping.

For both isotherms 2 and 3, the following general equation can be written

$$\sum_{i=1}^{N} \frac{K_i(\nu \rho_f y_i - \rho_s \Gamma_i)}{\gamma_i - \omega} + 1 = \left(\frac{\nu\delta}{\omega} - 1\right)\left[\sum_{i=1}^{N} \frac{\gamma_i \theta_i}{\gamma_i - \omega} - 1\right] + \chi \frac{\nu}{\omega} \tag{11}$$

where ν is any constant and $\chi \equiv \delta(1 - \Sigma\, \theta_i)$. For the Gurvitsch isotherm 2 we have $\delta = \delta_G$ and $\chi = 0$, while $\delta = \delta_L$ and $\chi = 1$ for isotherm 3.

Solution of a single TCC section

The material balance for a single TCC adsorption section can be written (Mazzotti et al., 1994) as

$$\frac{\partial}{\partial \xi}[m \rho_f y_i - \rho_s \Gamma_i] - \frac{\partial}{\partial \tau}[-\lambda \rho_f y_i - \rho_s \Gamma_i] = 0 \tag{12}$$

The parameter λ is defined as $\lambda \equiv \epsilon^*/(1-\epsilon_p)$ where $\epsilon^* \equiv \epsilon + (1-\epsilon)\epsilon_p$ is the total void in the system, ϵ_p is the intraparticle void in the composite solid phase. The relative fluid to solid flow ratio is collected in the parameter $m \equiv (u_f/u_s - \epsilon_p)/(1-\epsilon_p)$. Here we have defined m as the net volumetric flow ratio instead of a net mass-flow ratio as done previously (Mazzotti et al., 1994; Chiang, 1998). This is to single out the effect of fluid density in the following discussion.

With Eqs. 8 and 11, the material balance for a Gurvitsch system can be written as

$$\frac{\partial}{\partial \xi}\left[(m\delta_G - \omega) \prod_{i=2}^{N} (\Omega_i - \omega)\right] + \frac{\partial}{\partial \tau}\left[(\lambda \delta_G + \omega) \prod_{i=2}^{N} (\Omega_i - \omega)\right] = 0 \tag{13}$$

which applies to all values of ω. Taking the derivatives by part and substituting Ω_j or $m\delta_G$ for ω, we find

$$(m\delta_G - \Omega_j)\frac{\partial \Omega_j}{\partial \xi} + (\lambda \delta_G + \Omega_j)\frac{\partial \Omega_j}{\partial \tau} = 0, \quad \text{for } j = 2, N \tag{14}$$

$$\left[\prod_{k=2}^{N} (\Omega_k - m\delta_G)\right] \frac{\partial m\delta_G}{\partial \xi} = -\frac{\partial}{\partial \tau}\left[(\lambda \delta_G + \omega) \prod_{i=2}^{N} (\Omega_i - \omega)\right]_{\omega = m\delta_G} \tag{15}$$

At steady state, both $\partial \Omega_j/\partial \xi$ and $\partial(m\delta_G)/\partial \xi$ should be zero. Thus $m\delta_G$ and Ω_j should be position independent. Furthermore, the transient Eq. 14 leads to

$$\left(\frac{d\xi}{d\tau}\right)_{\Omega_j} = \frac{m\delta_G - \Omega_j}{\lambda \delta_G + \Omega_j} \tag{16}$$

This is exactly the same characteristic equation obtained previously for a constant selectivity stoichiometric system. Therefore, the steady-state solution of a nonstoichiometric Gurvitsch system satisfies the same constant state relationship discussed previously in Mazzotti et al. (1994) and Chiang (1998).

The term $m\rho_f y_i - \rho_s \Gamma_i \equiv f_i$ in the first bracket of Eq. 12 is the net flux of component i in a TCC section, and should be position-independent at steady state. By writing $f_i = m\rho_f y_i - \rho_s \Gamma_i^{\infty} \theta_i = (m\delta_G - \gamma_i)\theta_i/K_i$, we find that

$$m\delta_G \left[\sum_{i=1}^{N} \frac{f_i}{m\delta_G - \gamma_i}\right] = m\delta_G \left[\sum_{i=1}^{N} \frac{\theta_i}{K_i}\right] = m\rho_f \tag{17}$$

At steady state, everything on the lefthand side of Eq. 17 is position independent. Thus, $m\rho_f$ must also be position independent. However, the same may not be true for the volumetric flow ratio m or the fluid density ρ_f.

The situation is however different for systems following isotherm 3. For this case, the steady-state material balance becomes

$$\frac{\partial}{\partial \xi}\left[(m\delta_L-\omega)\prod_{i=1}^{N}(\Omega_i-\omega)-m\right]=0$$

or

$$\left[(m\delta_L-\Omega_j)\prod_{\substack{k=1\\k\neq j}}^{N}(\Omega_k-\Omega_j)\right]\frac{\partial\Omega_j}{\partial\xi}=\frac{\partial m}{\partial\xi} \tag{18}$$

$$\left[\sum_{k=1}^{N}(\Omega_k-m\delta_L)\right]\frac{\partial m\delta_G}{\partial\xi}=\frac{\partial m}{\partial\xi} \tag{19}$$

In general, all m, $m\delta_L$, and Ω_j vary with positions in the section, and it will be difficult to solve these equations analytically. As an approximation, Mazzotti et al. (1996) assumed that the volumetric flow ratio m is fixed, and forced the system to a constant state solution. However, if such an approximation is to be taken, it seems better to start with the Gurvitsch isotherm in the first place. In the following discussions, only the Gurvitsch isotherm 2 will be considered and the subscript G will be dropped from now on.

Complete Separation Conditions

We have proved that the steady-state solution of a nonstoichiometric Gurvitsch system is of the same form as a constant selectivity stoichiometric system reported previously (Chiang, 1998). All theorems developed there can now be applied. The most important step was the definition of a flux function $T(\omega)$. For the present case, it should be modified to

$$T(\omega)\equiv\sum_{i=1}^{N}\frac{K_i f_i}{\gamma_i-\omega}+1=\left(\frac{m\delta-\omega}{\gamma_1-\omega}\right)\sum_{i=2}^{N}\left(\frac{\Omega_i-\omega}{\gamma_i-\omega}\right) \tag{20}$$

Since $f_i=(m\delta-\gamma_i)\theta_i/K_i$, it is clear that $f_i<0$ if and only if $m\delta<\gamma_i$. Similarly, $0<f_i$ if and only if $\gamma_i<m\delta$, and $f_i=0$ if and only if θ_i or $m\delta-\gamma_i$ is zero. Having indexed the components according to increasing γ_i, all positive f_i will appear before negative ones. As in our previous article, one can also prove that $dT/d\omega<0$ if $m\delta<\gamma_1$, but $0<dT/d\omega$ if $\gamma_N<m\delta$. When $m\delta$ falls within $[\gamma_k,\ \gamma_{k+1}]$, $T(\omega)$ will have two roots $\omega^{\oplus}\leq\omega^{\ominus}$ in the same interval. One of them is the $m\delta$.

Following the convention used by Mazzotti et al. (1994), we will use the group R to represent the feed components desired in the raffinate outlet and the group E to represent those desired in the extract outlet. The strongest and the weakest components in groups R and E will be identified by subscripts Rs, Rw, Es, and Ew, respectively.

With these notations, the necessary and sufficient condition for a four-section TCC adsorption unit to achieve complete separation is (Chiang, 1998)

$$\begin{array}{llll} f_R^1=0, & f_R^2=0, & f_R^3=Fy_R^F, & f_R^4=0\\ f_E^1=0 & f_E^2=-Fy_E^F & f_E^3=0, & f_E^4=0\\ f_D^1>f_D^2 & f_D^2=f_D^3 & f_D^3=f_D^2 & f_D^3>f_D^4 \end{array} \tag{21}$$

where F is the mass-flow ratio of the feed stream and y_i^F is the feed compositions. Here, we have assumed that the desorbent input is free of any feed component, and the feed contains no desorbent. The objectives of the following analysis are to rephrase the above condition in terms of the operation parameters $m_1\rho_f$ to $m_4\rho_f$.

To do so, the first step is to rewrite the complete separation conditions in terms of the corresponding Ω-vectors. This has been given by Mazzotti et al. (1994) and was summarized in our previous article. The same condition applies here if we change the K_i to γ_i

$$\begin{aligned}\max\{\gamma_{Es},\Omega_D^{\beta}\}&\leq m_1\delta_1\\ m_4\delta_4&\leq\min\{\gamma_{Rw},\Omega_{D+1}^{d}\}\end{aligned} \tag{22}$$

and

$$\begin{array}{lll} \gamma_{Rs}\leq m_2\delta_2\leq\Omega_{Ew}^2 & \gamma_{Rs}<m_3\delta_3<\Omega_{Ew}^c & \text{if } \gamma_D<\gamma_{Rs}\\ \Omega_D^{\gamma}<m_2\delta_2\leq\Omega_{Ew}^2 & \Omega_D^3\leq m_3\delta_3<\Omega_{Ew}^c & \text{if } \gamma_{Rs}<\gamma_D<\gamma_{Ew}\\ \Omega_{Ew}^3<m_2\delta_2<\gamma_{Ew} & \Omega_{Ew}^3\leq m_3\delta_3\leq\gamma_{Ew} & \text{if } \gamma_{Ew}<\gamma_D \end{array} \tag{23}$$

Because sections 1 and 4 contain only the desorbent, it is clear that $\delta_1=\delta_4=K_D\rho_f$. The conditions on $m_1\rho_f$ and $m_4\rho_f$ can be explicitly written as

$$\max\{\gamma_{Es},\Omega_D^{\beta}\}/K_D\leq m_1\rho_f \tag{24}$$

$$m_4\rho_f\leq\min\{\gamma_{Rw},\Omega_{D+1}^{d}\}/K_D \tag{25}$$

Similar to Mazzotti et al. (1996).

Complete separation region on the $m_2\rho_f$-$m_3\rho_f$ plane

Given $m_1\rho_f$ and $m_4\rho_f$ values that satisfy Eqs. 24 and 25, the solution to the equilibrium model is now determined by $m_2\rho_f$ and $m_3\rho_f$. The procedure to find the complete separation region on $m_2\rho_f$-$m_3\rho_f$ plane will be the same as that presented previously for a stoichiometric system. First, a complete separation region is identified on the $\omega^{\oplus}$-$\omega^{\ominus}$ plane, where $\omega^{\oplus}$ and $\omega^{\ominus}$ are roots of the $T^2(\omega)$ or $T^3(\omega)$ functions. This $\omega^{\oplus}$-$\omega^{\ominus}$ region is then mapped to the f_D-F plane, and finally to the $m_2\rho_f$-$m_3\rho_f$ plane.

Because the same constant state solution applies to both a constant selectivity stoichiometric system and a nonstoichiometric Gurvitsch system, the complete separation region on the $\omega^{\oplus}$-$\omega^{\ominus}$ space is the same except the change of K_i to γ_i. It can be written as (Chiang, 1998)

$$\begin{aligned} &m_2\delta_2<\gamma_{Ew}\\ &\Omega_{Ew}^3=\omega_3^{\oplus}\leq\omega_3^{\ominus}=m_3\delta_3\leq\gamma_{Ew}\\ &\gamma_{Rs}<\Omega_{Ew}^3=\omega_3^{\oplus}\leq\min\{\Omega_{Ew}^F,\omega_3^{\ominus}\}\end{aligned} \tag{26}$$

for strong and intermediate-strong desorbents

$$\begin{aligned} &\gamma_{Rs}<m_3\delta_3\\ &\gamma_{Rs}\leq m_2\delta_2=\omega_2^{\oplus}\leq\omega_2^{\ominus}=\Omega_{Ew}^2\\ &\max\{\omega_2^{\oplus},\Omega_{Ew}^F\}\leq\omega_2^{\ominus}=\Omega_{Ew}^2<\gamma_{Ew}\end{aligned} \tag{27}$$

for weak and weak-intermediate desorbents, and either

$$m_2\delta_2 < \gamma_D$$
$$\gamma_{Rs} < \omega_3^{\oplus} = \Omega_D^3 \le \min\{\omega_3^{\ominus}, \Omega_D^F\}$$
$$\omega_3^{\oplus} \le \omega_3^{\ominus} = m_3\delta_3 < \gamma_D \tag{28}$$

or

$$\gamma_D < m_3\delta_3$$
$$\gamma_D < \omega_2^{\oplus} = m_2\delta_2 \le \omega_2^{\ominus}$$
$$\max\{\omega_2^{\oplus}, \Omega_{Ew}^F\} \le \omega_2^{\ominus} = \Omega_{Ew}^2 < \gamma_{Ew} \tag{29}$$

have to be true for intermediate desorbents. Each set of these relations defines a region on the $\omega_3^{\oplus}$-$\omega_3^{\ominus}$ or $\omega_2^{\oplus}$-$\omega_2^{\ominus}$ plane.

To map the $\omega^{\oplus}$-$\omega^{\ominus}$ complete separation region to the f_D-F plane, the relations

$$-\left(\frac{f_D^3}{F}\right) = \sum_R \left(\frac{\omega_3^{\oplus}-\gamma_D}{\omega_3^{\oplus}-\gamma_i}\right)\left(\frac{\omega_3^{\ominus}-\gamma_D}{\omega_3^{\ominus}-\gamma_i}\right)\left(\frac{K_i}{K_D}y_i^F\right) \tag{30}$$

$$\frac{1}{F} = \sum_R \frac{(\gamma_D-\gamma_i)K_i y_i^F}{(\omega_3^{\oplus}-\gamma_i)(\omega_3^{\ominus}-\gamma_i)} \tag{31}$$

$$\left(\frac{f_D^2}{F}\right) = \sum_E \left(\frac{\gamma_D-\omega_2^{\oplus}}{\gamma_i-\omega_2^{\oplus}}\right)\left(\frac{\gamma_D-\omega_2^{\ominus}}{\gamma_i-\omega_2^{\ominus}}\right)\left(\frac{K_i}{K_D}y_i^F\right) \tag{32}$$

$$\frac{1}{F} = \sum_E \frac{(\gamma_i-\gamma_D)K_i y_i^F}{(\gamma_i-\omega_2^{\oplus})(\gamma_i-\omega_2^{\ominus})} \tag{33}$$

will be used. These equations are identical to those given for stoichiometric systems, except the replacement of K_i to γ_i in some places.

Up to now, the procedure has been almost the same as that for a stoichiometric system. However, both γ_i and K_i now appear explicitly in Eqs. 30 to 33. The mapping from $\omega^{\oplus}$-$\omega^{\ominus}$ space to f_D-F space will thus depend on both γ_i and K_i. This is demonstrated in Figure 2 for the case of a strong desorbent. The complete separation region on the $\omega^{\oplus}$-$\omega^{\ominus}$ plane is the same as long as γ_i are fixed, but different images on the f_D-F plane are obtained if K_D is altered under a fixed γ_D. Knowing that $K_D f_D^3 \to (\omega_3^{\ominus}-\gamma_D)$ and $F \to 0$ as $\omega_3^{\oplus} \to \gamma_{Rs}$, one could have shifted the different f_D-F regions to the same position by using $K_D f_D^3 - \gamma_D$ as the abscissa instead.

The last step is to map the f_D-F complete separation region to the $m_2\rho_f$-$m_3\rho_f$ plane. This is where a nonstoichiometric system becomes different. To do so, let us rewrite Eq. 17 as

$$m_2\rho_f = \frac{m_2\delta_2}{m_2\delta_2-\gamma_D}f_D^2 - F\sum_E \frac{m_2\delta_2 y_i^F}{m_2\delta_2-\gamma_i} = F\left[\frac{f_D^2}{F} - \sum_E y_i^F\right] + F\left[\frac{\gamma_D}{m_2\delta_2-\gamma_D}\frac{f_D^2}{F} - \sum_E \frac{\gamma_i y_i^F}{m_2\delta_2-\gamma_i}\right] \tag{34}$$

and

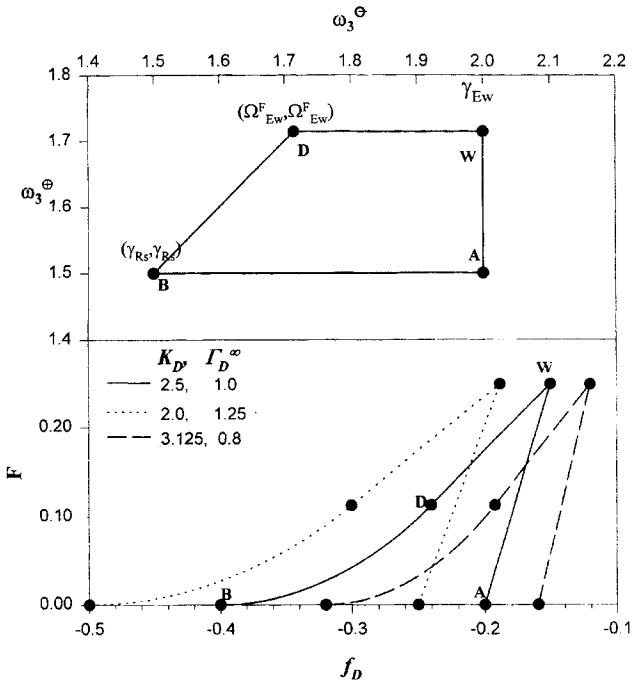

Figure 2. Same complete separation region is generated for a strong desorbent on the $\omega_3^{\oplus}$-$\omega_3^{\ominus}$ plane, but its image on the f_D-F plane varies with K_D even though the γ_D is the same.

The other parameters are $K_{R1}=1$, $K_{R2}=1.5$, $K_{E1}=2.0$, $K_{E2}=3.0$, $y_{R1}^F=0.25$, $y_{R2}^F=0.25$, $y_{E2}^F=0.2$, $y_{F2}^F=0.3$ and all Γ_i^{∞} except Γ_D^{∞} are 1.

$$m_3\rho_f = \frac{m_3\delta_3}{m_3\delta_3-\gamma_D}f_D^3 + F\sum_R \frac{m_3\delta_3 y_i^F}{m_3\delta_3-\gamma_i} = F\left[\frac{f_D^3}{F} + \sum_R y_i^F\right] + F\left[\frac{\gamma_D}{m_3\delta_3-\gamma_D}\frac{f_D^3}{F} + \sum_R \frac{\gamma_i y_i^F}{m_3\delta_3-\gamma_i}\right] \tag{35}$$

Notice that the second bracketed term in these equations always reduces to $\rho_s\Gamma^{\infty}$ if $\Gamma_i^{\infty}=\Gamma^{\infty}$. Therefore, for stoichiometric systems, the mapping from f_D-F space to $m_2\rho_f$-$m_3\rho_f$ space is nothing but a rotation of the axes.

For nonstoichiometric systems, however, the $m_2\delta_2$ and $m_3\delta_3$ terms involved in Eqs. 34 and 35 must be known to determine $m_2\rho_f$ and $m_3\rho_f$ for given f_D and F values. For a strong desorbent, $m_3\delta_3=\omega_3^{\ominus}$ according to condition 26. The $m_2\delta_2$, on the other hand, must be obtained separately by solving the equation $T^2(m_2\delta_2)=0$ with the given f_D^3 and F values. Since $f_D^3=f_D^2<0$, all nonvanishing net fluxes in section 2 are negative. $T^2(\omega)$ has exactly one root smaller than γ_{Ew}, which is the $m_2\delta_2$ desired.

With $m_2\delta_2$ and $m_3\delta_3$ found for each (f_D,F) point, the complete separation regions given in Figure 2 can be mapped to the $m_2\rho_f$-$m_3\rho_f$ plane as shown in Figure 3 by Eqs. 34 and 35. Notice that we have used $K_D m_2\rho_f$ and $K_D m_3\rho_f$ as the axes in this figure. Because $F\to 0$, $K_D f_D^3 \to (\omega_3^{\ominus}-\gamma_D)$ and $m_2\delta_2 \to \omega_3^{\ominus}$ when $\omega_3^{\oplus}\to\gamma_{Rs}$, both $K_D m_2\rho_f$ and $K_D m_3\rho_f$ should approach $\omega_3^{\ominus}$ when $\omega_3^{\oplus}\to\gamma_{Rs}$. In other words, the coordinates of point A are always $(\gamma_{Rs},\gamma_{Rs})$ on the $K_D m_2\rho_f$-$K_D m_3\rho_f$ plane, while those of point B are always $(\gamma_{Ew},\gamma_{Ew})$.

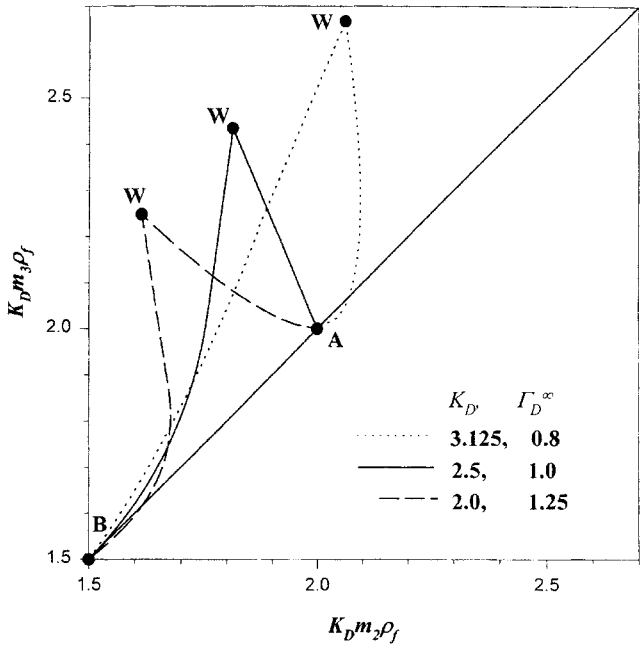

Figure 3. Image of the regions in Figure 2 on the m_2-m_3 plane.

Had we used $m_2 \rho_f$ and $m_3 \rho_f$ as the axes directly, the region with a larger K_D would have been at the lower corner and that with a smaller K_D would have been at the upper right corner.

By multiplying the axes with K_D, we have shifted the lower edge of the region to the same position, but the shape of the region is still different for different parameters. The triangular shaped region tilts to the right when the same γ_D is the product of a large K_D with a small Γ_D, and to the left when reversed. Such a behavior may be understood by inspecting the above equations; although the equilibrium constants K_i do not appear explicitly in Eqs. 34 and 35, they do so in the function $T^2(\omega)$. In other words, given f_D and F values, the root $m_2 \delta_2$ obtained depends on both γ_i and K_i. The change of $m_2 \delta_2$ then affects the shape of the region.

The tilting of the complete separation region can also be interpreted based on the previous results on stoichiometric systems. It has been found (Mazzotti et al., 1994; Chiang, 1998) that the triangular-shaped region always tilts to the right if the desorbent is strong and vice versa. Figure 3 thus suggests that the combination of a large K_D with a small Γ_D^∞ leads to a stronger desorbent than a small K_D with large Γ_D^∞. In other words, the equilibrium constant K_D is more important in determining the adsorptivity of the desorbent.

When K_D is large, the righthand boundary of the complete separation region in Figure 3 goes under the diagonal line and approaches point A from below. The same happens to the lefthand boundary when K_D is small. This behavior will be discussed later.

Given in Figure 4 is the complete separation region for a strong desorbent when K_D is kept constant, but Γ_D^∞ is varied. Since K_D is fixed, points A and B are fixed even when we have plotted the region on the $m_2 \rho_f$-$m_3 \rho_f$ plane. Here, we find that a smaller Γ_D^∞ increases the size of the complete separation region while a larger Γ_D^∞ decreases it. This is because we are dealing with a strong desorbent here. A smaller Γ_D^∞ weakens the strong desorbent, so that it is more like an intermediate one when the feed rate is high. A larger complete separation region is thus obtained. Conversely speaking, a larger Γ_D^∞ worsens the case and reduces the complete separation at a high feed rate. Therefore, although the adsorptivity of the desorbent is mostly determined by K_D, the saturation capacity Γ_D^∞ does modify its behavior at high feed rate.

For intermediate desorbent, the complete separation region on $\omega^{\oplus}$-$\omega^{\ominus}$ plane is defined by both relations 28 and 29, as demonstrated in Figure 5. This figure is the same as Figure 7 in Chiang (1998), but we have added here the relative magnitudes of $m\delta$ and θ_D in each subregion.

The same procedure is then applied to map the regions on Figure 5 to the $m_2 \rho_f$-$m_3 \rho_f$ space. The result is demonstrated in Figure 6 where γ_D is fixed but K_D is varied. In this figure we have used $m_2 \rho_f$ and $m_3 \rho_f$ as the axes without multiplying K_D, so that it is easier to compare with Figure 6 of Mazzotti et al. (1996). The general shape of the complete separation regions and their relative positions are similar to the result of Mazzotti et al., but our region boundaries again go across the diagonal line. Although the small portion of the region below the diagonal line is of no interest to the operation of the process, the correctness of this behavior needs to be verified.

Based on our definition of the component net flux, the total flux in a section is

$$\sum_{i=1}^{N} f_i = m\rho_f - \rho_s \sum_{i}^{N} \Gamma_i^\infty \theta_i \tag{36}$$

For a stoichiometric system, the second term reduces to $\rho_s \Gamma^\infty$. Therefore, the overall material balance of sections 2 and 3 leads to $m_3 \rho_f$-$m_2 \rho_f = F$. From this, we know that $m_3 \rho_f$

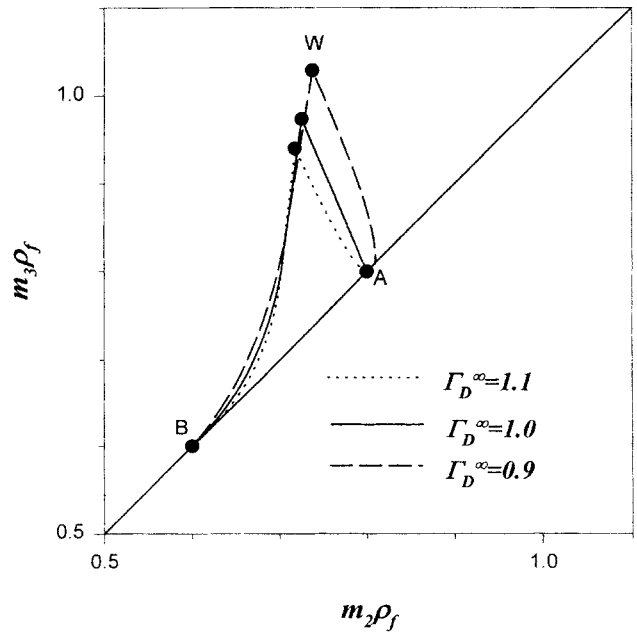

Figure 4. Variation of m_2-m_3 complete separation region with Γ_D^∞ while K_D = 2.5.

All other parameters are the same as Figure 2.

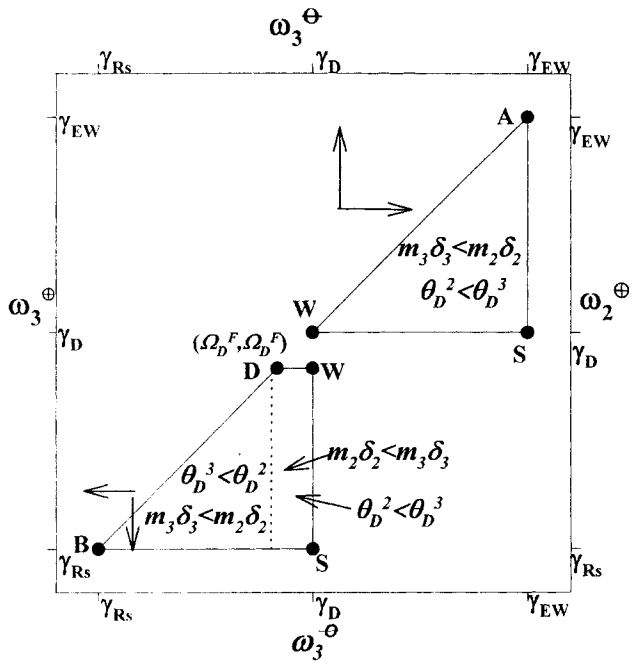

Figure 5. Complete separation region on the $\omega^{\oplus}$-$\omega^{\ominus}$ plane for an intermediate desorbent.

This is for the case where $\Omega_D^F < \gamma_D$. If $\gamma_D < \Omega_{D+1}^F$, the ω_2 region will be a tetragonal and the ω_3 region will be a triangle.

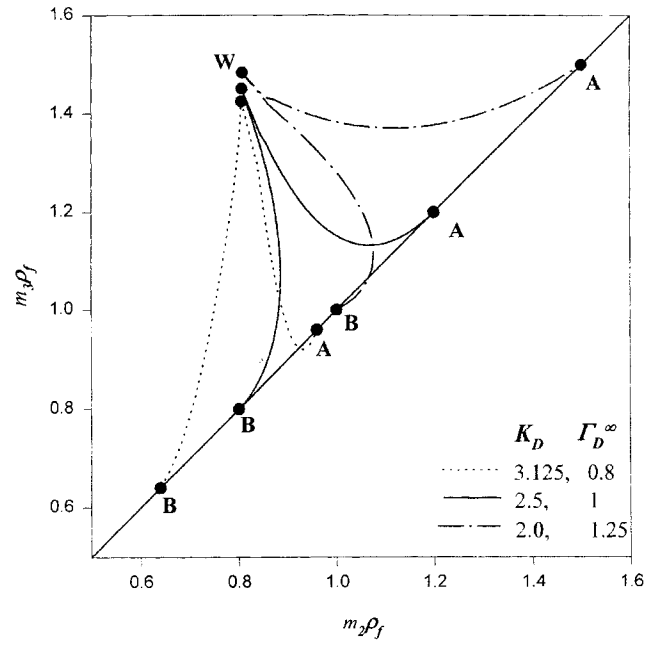

Figure 6. Complete separation region on the m_2-m_3 plane for an intermediate desorbent.

Parameters are $K_{R1}=1$, $K_{R2}=1.5$, $K_{R3}=2.0$, $K_{E1}=3.0$, $y_{R1}^F=0.25$, $y_{R2}^F=0.25$, $y_{R3}^F=0.2$, $y_{E1}^F=0.3$. All Γ_i^{∞} except Γ_D^{∞} are 1.

should always be larger than $m_2\,\rho_f$. However, for a nonstoichiometric system we have

$$m_3\,\rho_f - m_2\,\rho_f = F - \rho_s\left(\sum_{E,D}\Gamma_i^{\infty}\theta_i^2 - \sum_{R,D}\Gamma_i^{\infty}\theta_i^3\right) \qquad (37)$$

There are two possibilities for $m_2\,\rho_f$ and $m_3\,\rho_f$ to be equal. The first case is when $F=0$; thus, all θ_i but θ_D become zero. However, if more adsorbates are carried to the left by the solid plase in section 2 than in section 3, the bracketed term on the righthand side may become positive, and we may have $m_3\,\rho_f < m_2\,\rho_f$ at small F. This is most likely to happen if $\Gamma_E^{\infty} \gg \Gamma_R^{\infty}$.

For the cases shown in Figures 3 and 6, we have $\Gamma_R^{\infty}=\Gamma_E^{\infty}=\Gamma^{\infty}$ and the above equation reduces to

$$m_3\,\rho_f - m_2\,\rho_f = F - \rho_s(\Gamma_D^{\infty}-\Gamma^{\infty})(\theta_D^2-\theta_D^3) \qquad (38)$$

With $\Gamma^{\infty}<\Gamma_D^{\infty}$, $m_3\,\rho_f$ may be smaller than $m_2\,\rho_f$ if $\theta_D^3<\theta_D^2$. This happens only in the lower triangle region shown in Figure 5. When $\Gamma_D^{\infty}<\Gamma^{\infty}$, $m_3\,\rho_f$ may be smaller than $m_2\,\rho_f$ if $\theta_D^2<\theta_D^3$, or when the $(m_2\delta_2,\ m_3\delta_3)$ point is near point A. This is exactly what was observed in Figures 3 and 6.

The point marked as W in Figure 6 corresponds to the optimal operating condition predicted by the equilibrium theory for an intermediate desorbent. For the parameters used in this figure, we have $\Omega_D<\gamma_D$, and the point W corresponds to $\omega_3^{\oplus}=\Omega_D$ and $\omega_3^{\ominus}=\gamma_D$. The coordinates for point W are therefore

$$\rho_f m_2 = \left[\sum_E y_i^F - \sum_E \frac{\gamma_i y_i^F}{\gamma_i-\Omega_D^F}\right]\Bigg/\left[\sum_E \frac{K_i y_i^F}{\Omega_D^F-\gamma_i}\right] \qquad (39)$$

$$\rho_f m_3 = \left[\sum_R y_i^F + \sum_R \frac{\gamma_i y_i^F}{\Omega_D^F-\gamma_i}\left(\frac{\Gamma_D^{\infty}}{\Gamma_i^{\infty}}\right) + \sum_R \frac{\gamma_i y_i^F}{\gamma_D-\gamma_i}\left(1-\frac{\Gamma_D^{\infty}}{\Gamma_i^{\infty}}\right)\right]\Bigg/\left[\sum_R \frac{K_i y_i^F}{\Omega_D^F-\gamma_i}\right] \qquad (40)$$

They reduce exactly to the Eqs. 42 and 43 in Chiang (1998) when $\Gamma_i^{\infty}=\Gamma^{\infty}$.

In summary, the procedure developed previously for finding the complete separation region in the m_2-m_3 space also works for nonstoichiometric Gurvitsch systems. The procedure is practically the same except that the mapping from f_D-F space to $m_2\,\rho_f$-$m_3\,\rho_f$ space is slightly more complicated for nonstoichiometric Gurvitsch systems. Both the equilibrium constant K_i and the selectivity γ_i are involved in determining the complete separation region for a nonstoichiometric system, but the former seems to be more important in determining the adsorptivity of the components.

Partial Separation Regions

Storti et al. (1995) demonstrated that the operation parameter space (m_2, m_3) can be divided into regions of different separation regimes, where the separation may be incomplete. It is demonstrated that the approach given in previous sections also works when the separation is incomplete. To do so, let us redefine the group R to those components that are

excluded from the extract outlet, and the group E to components that are excluded from the raffinate outlet. A new group B will be used to represent components that go to both outlets. A complete separation is achieved when group B has no element. As in the other groups, the weakest and strongest components in group B will be identified by subscripts Bw and Bs, respectively. Each component in group B is further associated with a pair of recovery η_i^R and η_i^E. The η_i^R is the fraction of component i recovered in the raffinate outlet. The η_i^E is that recovered in the extract outlet. Therefore $\eta_i^R + \eta_i^E = 1$.

Let us assume that conditions 24 and 25 have already been met and y_D^E. Then, the net fluxes in columns 2 and 3 will be

$$\begin{aligned} f_R^2 &= 0 & f_R^3 &= F \cdot y_j^F \\ f_B^2 &= -F \cdot \eta_B^E y_B^F & f_B^3 &= F \cdot \eta_B^R y_B^F \\ f_E^2 &= -F \cdot y_E^F & f_E^3 &= 0 \\ f_D^2 &= f_D & f_D^3 &= f_D + F y_D^F \end{aligned} \tag{41}$$

and $T^2(\omega)$ and $T^3(\omega)$ can be written as

$$T^2(\omega) = 1 + \left(\frac{K_D}{\gamma_D - \omega}\right) f_D^2 - F\sum_E \frac{K_i y_i^F}{\gamma_i - \omega} - \sum_B \left(\frac{K_i y_i^F}{\gamma_i - \omega}\right) \eta_i^E F \tag{42}$$

$$T^3(\omega) = 1 + \left(\frac{K_D}{\gamma_D - \omega}\right) f_D^3 + F\sum_R \frac{K_i y_i^F}{\gamma_i - \omega} + \sum_B \left(\frac{K_i y_i^F}{\gamma_i - \omega}\right) \eta_i^R F \tag{43}$$

Because $f_D^2 < 0$ when $\gamma_{Bw} < \gamma_D$ but $f_D^3 > 0$ when $\gamma_D < \gamma_{Bs}$, one cannot have a situation with $\gamma_{Bw} < \gamma_D < \gamma_{Bs}$. The only possibilities are therefore $\gamma_{Bw} \le \gamma_{Bs} < \gamma_D$ and $\gamma_D < \gamma_{Bw} \le \gamma_{Bs}$.

For the case with $\gamma_{Bw} \le \gamma_{Bs} < \gamma_D$, the following conditions must be met so that Eq. 41 will be true

$$\Omega_{Bw}^F \le m_2\delta_2 < \gamma_{Bw} \tag{44}$$

$$\gamma_{Bs} < m_3\delta_3 \le \gamma_{Bs+1} \tag{45}$$

$$\begin{cases} T^3(\Omega_{Bs+1}^F) = 0 & \text{if } \Omega_{Bs+1}^F \le m_3\delta_3 \le \gamma_{Bs+1} \\ [dT^3/d\omega]_{m_3\delta_3} = 0 & \text{if } \gamma_{Bs} < m_3\delta_3 \le \Omega_{Bs+1}^F \end{cases} \tag{46}$$

and

$$T^3(\Omega_i^F) = 0 \quad \text{for} \quad i \in B,\ i \ne Bw \tag{47}$$

The proof for these conditions is given in the Appendix.

The relations 44 and 45 define a region on the $m_2\delta_2$-$m_3\delta_3$ plane. On the other hand, equalities 46 and 47, plus $T^2(m_2\delta_2) = T^3(m_3\delta_3) = 0$, form a set of $(Bs - Bw + 3)$ linear equations from which the variables f_D/F, $1/F$, and η_j^E can be solved for given values of $m_2\delta_2$ and $m_3\delta_3$. Once the f_D, F, and η_j^E are found, the net fluxes and compositions in sections 2 and 3 are completely specified. The corresponding values of $m_2\rho_f$ and $m_3\rho_f$ can then be found by

$$m_2\rho_f = \left[f_D - F\sum_E y_i^F - F\sum_B \eta_i^E y_i^F\right] + \left[\frac{\gamma_D f_D}{m_2\delta_2 - \gamma_D} - F\sum_E \frac{\gamma_i y_i^F}{m_2\delta_2 - \gamma_i} - F\sum_B \frac{\eta_i^E \gamma_i y_i^F}{m_2\delta_2 - \gamma_i}\right] \tag{48}$$

and

$$m_3\rho_f = \left[f_D + F\sum_R y_i^F + F\sum_B \eta_i^R y_i^F\right] + \left[\frac{\gamma_D f_D}{m_3\delta_3 - \gamma_D} + F\sum_R \frac{\gamma_i y_i^F}{m_3\delta_3 - \gamma_i} + F\sum_B \frac{\eta_i^R \gamma_i y_i^F}{m_3\delta_3 - \gamma_i}\right] \tag{49}$$

Let us recapitulate the procedure described above. By identifying the components in groups R, E and B, a region on the $m_2\delta_2$-$m_3\delta_3$ is specified by Eqs. 44 and 45. For every $(m_2\delta_2,\ m_3\delta_3)$ point in this region, a set of f_D, F and η_i^R values can be solved from Eqs. 46 and 47 plus $T^2(m_2\delta_2) = T^3(m_3\delta_3) = 0$. From these, the corresponding $(m_2\rho_f,\ m_3\rho_f)$ point can be found. In other words, the region on the $m_2\delta_2$-$m_3\delta_3$ plane is first mapped to a $(f_D,\ F,\ \eta_i^R)$ space, and then to the $m_2\rho_f$-$m_3\rho_f$ plane.

Shown in Figure 7 is an example of the $m_2\delta_2$-$m_3\delta_3$ region defined by conditions 44 and 45, as well as its image on the

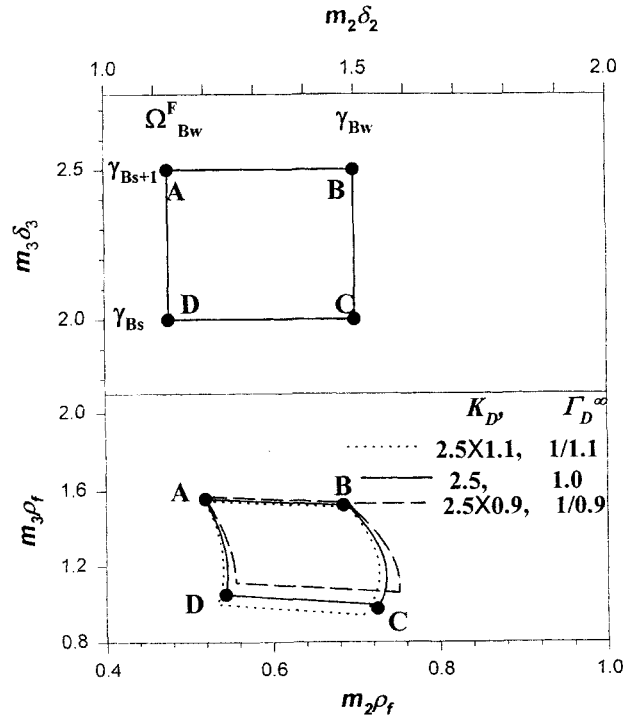

Figure 7. Partial separation region on the $m_2\delta_2$-$m_3\delta_3$ and m_2-m_3 planes.

The parameters are $K_B = 1$, $K_{Bw} = 1.5$, $K_{Bs} = 2.0$, $K_E = 3.0$, $y_R^F = 0.25$, $y_{Bw}^F = 0.25$, $y_{Bs}^F = 0.2$, $y_E^F = 0.3$. All Γ_i^∞ except Γ_D^∞ are 1.

$m_2\rho_f$-$m_3\rho_f$ plane. Again, the $m_2\delta_2$-$m_3\delta_3$ region is a function of the γ_i only, but its image on the $m_2\rho_f$-$m_3\rho_f$ plane depends on both γ_i and K_i. As shown in Figure 7, the $m_2\rho_f$-$m_3\rho_f$ region is shifted to the lower-left corner when K_D is increased under a fixed γ_D.

The procedures are similar when $\gamma_D < \gamma_{Ew} \le \gamma_{Rs}$. The appropriate region on the $m_2\delta_2$-$m_3\delta_3$ plane is defined by

$$\gamma_{Bs} < m_3\delta_3 \le \Omega^F_{Bs+1} \tag{50}$$

$$\gamma_{Bw-1} \le m_2\delta_2 < \gamma_{Bw} \tag{51}$$

and the equalities to be solved are $T^2(m_2\delta_2) = T^3(m_3\delta_3) = 0$,

$$\begin{cases} [dT^2/d\omega]_{m_2\delta_2} = 0 & \Omega^F_{Bw} \le m_2\delta_2 < \gamma_{Bw} \\ \text{if} & \\ T^2(\Omega^F_{Bw}) = 0 & \gamma_{Bw-1} \le m_2\delta_2 \le \Omega^F_{Bw} \end{cases} \tag{52}$$

and

$$T^2(\Omega^F_i) = T^3(\Omega^F_i) = 0 \qquad Bw \le i < Bs \tag{53}$$

To divide the $m_2\rho_f$-$m_3\rho_f$ plane into regions of different separation regimes, one has to go through all possible combinations for components in groups R, E and B. For each case, a $m_2\delta_2$-$m_3\delta_3$ region is first found. It is then mapped to the $m_2\rho_f$-$m_3\rho_f$ plane. A map that partitions the $m_2\rho_f$-$m_3\rho_f$ plane into different separation regimes can then be generated, as demonstrated in Figure 8. Since the mapping from $m_2\delta_2$-$m_3\delta_3$ space to $m_2\rho_f$-$m_3\rho_f$ space is one-to-one, only the region boundaries need to be calculated. Furthermore,

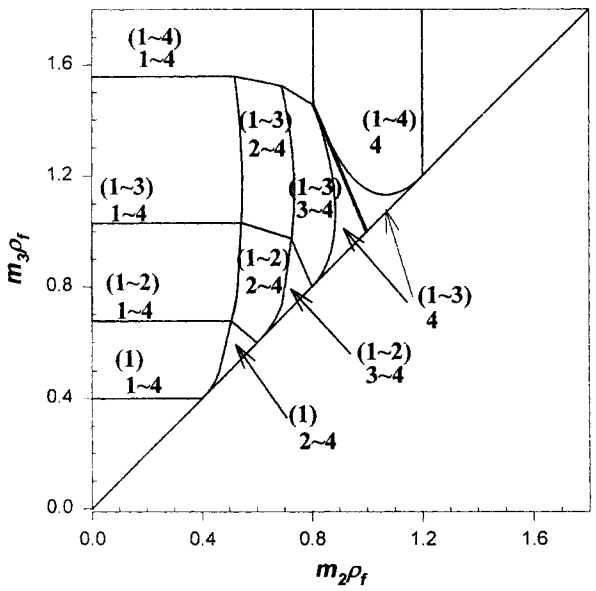

Figure 8. Different separation regions on the m_2-m_3 plane.

Number in the parentheses indicates that the components appear in the raffinate outlet. Number without parentheses indicates that the components appear in the extract outlet. The parameters are the same as in Figure 7.

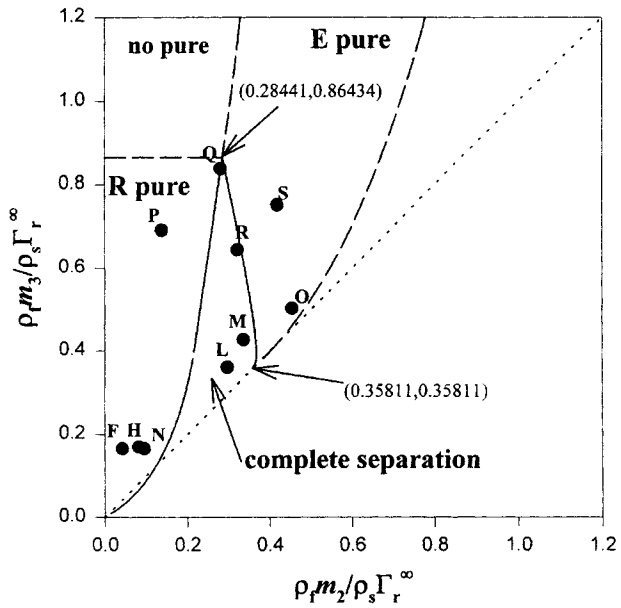

Figure 9. Separation regions for the *n*/isopentane separation system.

Parameters were $K_1 = 3.0$, $K_2 = 9.1$, $K_D = 27$, $\Gamma_1^\infty = 0.03$, $\Gamma_2^\infty = 0.85$, $\Gamma_D^\infty = 0.7$. The points are the experimental data reported by Mazzotti et al. (1996).

the common boundary shared by neighboring regions needs to be calculated only once.

In calculating the region boundary, limiting values of $m\delta$ are sometimes required. For example, we have $\eta^E_{Bw} \to 0$ when $m_2\delta_2 \to \gamma_{Bw}$ and $\eta^R_{Bs} \to 0$ when $m_3\delta_3 \to \gamma_{Bs}$. At these limiting cases, both the number of linear equations and the variables to be solved are reduced by one.

Special attention should be given to cases where the group R contains no element. This is when all feed components appear in the extract outlet. For this case, the $m_2\rho_f = 0$ line is a boundary for the region on the $m_2\rho_f$-$m_3\rho_f$ plane. Furthermore, $T^3(\omega)$ is now an explicit function of f^3_D and $F\eta^B_i$. These variables can be solved without the equation $T^2(m_2\delta_2) = 0$, and are thus independent of $m_2\delta_2$. In other words, the boundaries where $m_3\delta_3 \to \gamma_{Bs}$ or γ_{Bs+1} are independent of $m_2\rho_f$, and are, thus, horizontal lines on the $m_2\rho_f$-$m_3\rho_f$ plane. A similar situation applies to cases where the group E has no element. For such case, the $m_2\delta_2 \to \gamma_{Bw-1}$ or γ_{Bw} boundaries are vertical lines on the $m_2\rho_f$-$m_3\rho_f$ plane.

Example

Let us take the *n*/isopentane separation discussed by Mazzotti et al. (1996) as an illustration to further demonstrate the analytical solutions described above. Due to the molecular sieving effect, isopentane is nearly excluded from the 5A zeolite used as adsorbent in this system. This is evident from the extremely small saturation capacity for isopentane listed under Figure 9. These parameters have been taken from Mazzotti et al. (1996) where the isotherm 3 was employed. We assumed that the same constants can be used for a Gurvitsch isotherm, because the factor of 1 in the denominator is insignificant compared to the summation term for most cases.

Take the subscripts 1, 2, and D for the iso-, n-pentane, and n-heptane desorbent, respectively. To achieve any separation, the flow ratios in sections 1 and 4 must be such that $\Omega_D^{\beta} \le K_D \rho_f m_1$ and $K_D \rho_f m_4 \le \gamma_1$. With these conditions satisfied, the complete separation region on the $m_2 \rho_f$-$m_3 \rho_f$ plane can be found from the mapping of $\gamma_1 < \omega_3^{\oplus} \le \omega_3^{\ominus} \le \gamma_2$ with the help of Eqs. 30, 31, 34, and 35. The result is given in Figure 9. The combination of $m \rho_f / \rho_s \Gamma_r^{\infty}$ in our notation corresponds to the m value in their notation.

Our results are somewhat different from those obtained by Mazzotti et al. (1996). First of all, the lefthand boundary of the complete separation region goes below the diagonal line, and the righthand boundary curves as it approaches the diagonal line. Similar behavior has been demonstrated in Figures 3 and 6. For the present case, the saturation capacity of isopentane is twenty times smaller than that of n-pentane and n-heptane. In other words, the bracketed term on the righthand side of Eq. 37 is positive most of the time, and $m_3 \rho_f$ will be smaller than $m_2 \rho_f$ when F is small.

According to our solution, the lower bound for the pure raffinate region should be at $K_D \rho_f m_3 = \gamma_1$. Since $\gamma_1 \ll K_D \rho_f$, it is effectively the origin of the axes as Mazzotti et al. (1996) have found. However, our upper bound for the pure raffinate region is different from theirs. Our solution suggests a horizontal boundary at

$$K_D \rho_f m_3 = \gamma_2 \left[\left(\frac{K_D}{K_1} \right) \left(\frac{\Omega_2^F - \gamma_1}{\gamma_D - \gamma_1} \right) + \left(\frac{\gamma_D - \Omega_2^F}{\gamma_D - \gamma_1} \right) \right] \quad (54)$$

or $\rho_f m_3 / \rho_s \Gamma_r^{\infty} = 0.86434$, but their boundary had a positive slope.

The experimental data reported by Baciocchi et al. (1996) are also marked in Figure 9. Although the region boundaries we predicted are somewhat different from those of Mazzotti et al., all points except Q are still located in the correct region. Point Q, on the other hand, is located almost on the vertex of the complete separation region we have predicted, but is clearly more to the pure raffinate side. If our prediction is correct, one would observe a pure raffinate with a contaminated extract, but this contradicts the experimental finding. Instead, the extract was pure but the raffinate was not.

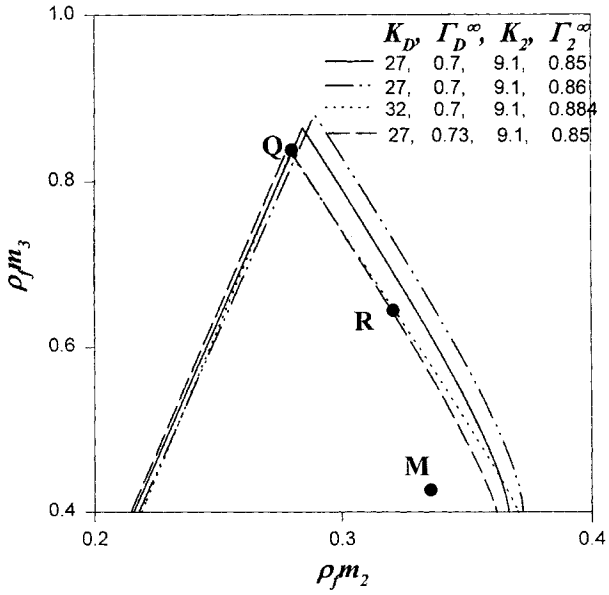

Figure 10. Variation of complete separation region upon small changes in the parameters for the example case shown in Figure 9.

Since point Q is so close to the vertex of the triangle, a small change of the system parameters may shift the vertex to the other side. The variation of the complete separation region upon changing the equilibrium parameters is demonstrated in Figure 10 with magnification. According to these tests, it seems that the saturation capacity of the desorbent used to calculate Figure 9 might have been underestimated.

Conclusions

Our previous technique for solving the equilibrium model of a TCC adsorption unit has been extended to systems following a nonstoichiometric adsorption isotherm. The key to our technique is again the flux function $T(\omega)$. In here, its definition has been modified.

The exact analysis of the nonstoichiometric equilibrium model presented here is more than finding the complete separation region on the parameter space. The same technique can be used to identify the operation parameter so that a partial separation can be achieved. Therefore, a map can be generated on the $m_2 \rho_f$-$m_3 \rho_f$ plane that describes the operation conditions leading to different kinds of separation results.

The procedure described in this article is fundamentally different from the usual ways to solve a model. Typically, the state of the system is solved from a model with all operation parameters given. In here, we are solving for the operation parameters that lead to a specified outcome. Because there are less operation parameters than system variables, the problem is actually easier. However, one has to analyze the problem differently.

It should be pointed out that the adsorption isotherm assumed in this article is different from the one employed by Mazzotti et al. (1996). For the type of isotherm assumed here, the composition in each TCC section is position independent at steady state. For the isotherm used by Mazzotti et al., the composition will be position dependent and the problem is much more difficult.

An important conclusion has been obtained from the example cases studied. The adsorptivity of the components is largely determined by the equilibrium constants K_i, but will be modified by the saturation capacity Γ_i^{∞} when the feed rate is high. If the desorbent is a strong one, that is, $K_{Ew} < K_D$, a smaller Γ_D^{∞} helps to bring the desorbent closer to an intermediate one, and vice versa.

Acknowledgment

This research has been supported by a grant from SM Corporation in Taiwan.

Notation

f_j^i = normalized net flux of component i in stream (section) j
K_i = the equilibrium constant of component i (m^3/mol)
L = the length of a TCC adsorption section

m_i = net volumetric flow ratio in section i, defined as $(u_f/u_s - \epsilon_p)/(1 - \epsilon_p)$
t = time
u = superficial fluid phase velocity
u_s = superficial solid phase velocity
z = axial coordinate
δ = equilibrium theory parameter, $\delta_G \equiv \Sigma K_i \rho_f y_i$, $\delta_L \equiv 1 + \Sigma K_i \rho_f y_i$
ϵ_p = intraparticle void fraction
ϵ^* = overall void fraction, $\epsilon^* = \epsilon + \epsilon_p(1 - \epsilon)$
Γ_i^∞ = adsorbed phase saturation capacity of component i
ρ_f = fluid phase molar density
τ = dimensionless time, $\tau = tu_s/L$
ξ = dimensionless position, $\xi \equiv z/L$
$\chi = \delta(1 - \Sigma\theta_i)$. $\chi = 0$ for isotherm 2 and $\chi = 1$ for isotherm 3

Literature Cited

Baciocchi, R., M. Mazzotti, G. Storti, and M. Morbidelli, "C5 Separation in a Vapor Phase Simulated Moving Bed Unit," *Fundamental of Adsorption*, M. D. LeVan, ed., Kluwer Academic Publ., Boston, p. 95 (1996).

Chiang, A. S. T., "Complete Separation Conditions for a Local Equilibrium TCC Adsorption Unit," *AIChE J.*, **44**, 332 (1998).

Gurvitsch, L., *J. Phys. Chem. Soc. Russ.*, **47**, 805 (1915).

Hotier, G., "Physically Meaningful Modeling of 3-Zone and 4-Zone Simulated Moving Bed Processes," *AIChE J.*, **42**, 154 (1996).

Minka, C., and A. L. Myers, "Adsorption from Ternary Liquid Mixture on Solids," *AIChE J.*, **19**, 453 (1973).

Mazzotti, M., G. Storti, and M. Morbidelli, "Robust Design of Countercurrent Adsorption Separation Processes: 2. Multicomponent Systems," *AIChE J.*, **40**, 1825 (1994).

Mazzotti, M., G. Storti, and M. Morbidelli, "Robust Design of Countercurrent Adsorption Separation Processes: 3. Non-Stoichiometric Systems," *AIChE J.*, **42**, 2784 (1996).

Mazzotti, M., G. Storti, and M. Morbidelli, "Robust Design of Countercurrent Adsorption Separation Processes: 4. Desorbent in the Feed," *AIChE J.*, **43**, 64 (1997).

Rhee, H. K., R. Aris, and N. Amundson, "Multicomponent Adsorption in Continuous Countercurrent Exchangers," *Phil. Trans. Roy. Soc. London*, **A269**, 187 (1971).

Rhee, H. K., R. Aris, and N. Amundson, *First-Order Partial Differential Equations*, Vol. II, Prentice Hall, Englewood Cliffs, NJ (1989).

Rota, R., G. Gamba, and M. Morbidelli, "On the Use of the Adsorption Solution Theory for Designing Adsorption Separation Units," *Sep. Technol.*, **3**, 230 (1993).

Ruthven, D. M., and C. B. Ching, "Countercurrent and Simulated Countercurrent Adsorption Separation Process," *Chem. Eng. Sci.*, **44**, 1011 (1989).

Storti, G., M. Masi, S. Carra, and M. Morbidelli, "Optimal Design of Multicomponent Countercurrent Adsorption Separation Processes Involving Nonlinear Equilibria," *Chem. Eng. Sci.*, **44**, 1329 (1989).

Storti, G., M. Mazzotti, M. Morbidelli, and S. Carra, "Robust Design of Binary Countercurrent Adsorption Separation Processes," *AIChE J.*, **39**, 471 (1993).

Storti, G., R. Baciocchi, M. Mazzotti, and M. Morbidelli, "Design of Optimal Operating Conditions of Simulated Moving Bed Adsorptive Separation Units," *Ind. Eng. Chem. Res.*, **34**, 288 (1995).

Talu, O., J. Li, and A. L. Myers, "Activity Coefficients of Adsorbed Mixture," *Adsorption*, **1**, 103 (1995).

Appendix

Let us first prove the inequalities 44 for the case where $\gamma_{Bw} \le \gamma_{Bs} < \gamma_D$. For section 2, $f_{Bs}^2 < 0$ leads to $f_D^2 = f_D^3 \le 0$. For section 3, f_{Bs}^3 must be positive but we have proved $f_D^3 \le 0$. Therefore, $T^3(\omega)$ should have two roots $\omega_3^\oplus \le \omega_3^\ominus$ in the interval $[\gamma_{Bs}, \gamma_D]$. One of them is $m_3\delta_3$ and the other is Ω_{Bs+1}^3. We shall next prove that both $m_3\delta_3$ and Ω_{Bs+1}^3 are smaller than or equal to γ_{Bs+1}.

According to the theorem

$$\min\{\Omega_i^D, \Omega_i^F\} \le \Omega_i \le \max\{\Omega_i^D, \Omega_i^F\} \tag{A1}$$

given by Mazzotti et al. (1994), we have $\gamma_{Bs} = \Omega_{Bs+1}^D \le \Omega_{Bs+1}^3 \le \Omega_{Bs+1}^F < \gamma_{Bs+1}$. The first equality comes from the fact that $\gamma_{Bs} < \gamma_D$, and there are no feed components in the desorbent input. We have thus proved that $\Omega_{Bs+1}^3 < \gamma_{Bs+1}$. To prove that $m_3\delta_3 \le \gamma_{Bs+1}$, we will use the fact that $f_{Bs+1}^3 = 0$ and thus $\gamma_{Bs+1} \in \Omega^3$. If $\gamma_{Bs+1} < m_3\delta_3$, then $\gamma_{Bs+1} \in \Omega^\gamma$ according to the constant state relationship. This cannot be true since f_{Bs+1}^γ cannot be zero. Therefore, $m_3\delta_3 \le \gamma_{Bs+1}$.

The next thing to prove is that $\omega_3^\oplus = \Omega_{Bs+1}^3$ and $\omega_3^\ominus = m_3\delta_3$. If $\omega_3^\oplus = m_3\delta_3 < \omega_3^\ominus = \Omega_{Bs+1}^3 \le \Omega_{Bs+1}^F$, the constant state relations require that the root Ω_{Bs+1}^3 be inherited from the right, or from stream δ. In other words, $\omega_3^\ominus = \Omega_{Bs+1}^d = \Omega_{Bs+1}^\delta = \Omega_{Bs+1}^4$. This cannot be true since section 4 contains only the desorbent. Therefore, we must have

$$\gamma_{Bs} = \omega_3^\oplus = \Omega_{Bs+1}^3 \le \min\{\Omega_{Bs+1}^F, m_3\delta_3\} \le \omega_3^\ominus = m_3\delta_3 \le \gamma_{Bs+1}$$

Notice that the same procedures can also be used to prove relation 26 if one replaces the subscript $Bs+1$ by $Rs+1$.

The upper bound for $m_2\delta_2$ in the inequality 45 is easily proved knowing that all nonvanishing net fluxes in section 2 are negative, thus $m_2\delta_2 < \gamma_{Bw}$, and $T^2(\omega)$ must be a decreasing function for all ω. However, the lower bound for $m_2\delta_2$ has to be dealt with after we prove equalities 46 and 47.

Knowing that $m_2\delta_2 < \gamma_{Bw}$, it is clear that $\Omega_i^2 = \Omega_i^\gamma = \Omega_i^c$ for all $i > Bw$. Since $\Omega_{Bs+1}^3 = \omega_3^\oplus$ and $m_3\delta_3 = \omega_3^\ominus$, $m_3\delta_3$ can either be larger than Ω_{Bs+1}^3 or equal to it. When $\Omega_{Bs+1}^3 < m_3\delta_3$, we have $\Omega_{Bs+1}^\gamma = \Omega_{Bs+1}^3$. However, Ω_{Bs+1}^2 also is equal to Ω_{Bs+1}^γ; thus, $\Omega_{Bs+1}^2 = \Omega_{Bs+1}^3 = \Omega_{Bs+1}^F$ and $T^3(\Omega_{Bs+1}^F) = 0$. This is the first half of Eq. 46. If Ω_{Bs+1}^3 and $m_3\delta_3$ are equal, they are double root to the function $T^3(\omega)$; thus, the second half of Eq. 46 must be true.

To prove Eq. 47, consider the fact that $T^2(\omega)$ is a decreasing function for all ω. Since $\Omega_i^2 \le \Omega_i^F$ for $Bw < i \le D$ according to Eq. A1, we have $T^2(\Omega_i^F) \le 0$. On the other hand, all nonvanishing in section 3 are positive and $T^3(\omega)$ is an increasing function for all ω. We have $T^3(\Omega_i^F) \ge 0$ for $i \le Bs$. However, $T^2(\Omega_j^F) = T^3(\Omega_j^F)$ must always be true. Therefore, Eq. 47 is proved.

Finally, from $T^2(\Omega_{Bw}^F) = T^3(\Omega_{Bw}^F) \ge 0$ and that $T^2(\omega)$ is a decreasing function, we can prove the lower bound for $m_2\delta_2$ in Eq. 45, that is, $\Omega_{Bw}^F \le m_2\delta_2$.

Manuscript received Dec. 1, 1997, and revision received Aug. 4, 1998.